Paredes Paredes, M. C., Escudero-Garzas, J. J. & Fernandez-Getino Garcia, M. J. (2016). PAPR Reduction via Constellation Extension in OFDM Systems Using Generalized Benders Decomposition and Branch-and-Bound Techniques. *IEEE Transactions on Vehicular Technology*, 65(7), pp. 5133–5145.

DOI: 10.1109/tvt.2015.2450178

PAPR reduction via Constellation Extension in OFDM systems using Generalized Benders Decomposition and Branch and Bound techniques

Martha C. Paredes Paredes, *Member, IEEE,* J. Joaquín Escudero-Garzás, *Member, IEEE,* and M. Julia Fernández-Getino García, *Member, IEEE*

***Abstract*—In this paper, a novel Constellation Extension (CE) based approach is presented to address the high Peak-to-Average Power Ratio (PAPR) problem at the transmitter side, which is an important drawback of Orthogonal Frequency Division Multiplexing (OFDM) systems. This new proposal is formulated as a Mixed Integer Non-Linear Programming (MINLP) optimization problem, which employs Generalized Benders Decomposition (GBD) and Branch-and-Bound (BB) methods to determine the most adequate extension factor and the optimum set of input symbols to be extended within a proper quarter-plane of the constellation. The optimum technique based on GBD, denoted as Generalized Benders Decomposition for Constellation Extension (GBDCE), provides a bound with relevant improvement in terms of PAPR reduction compared with other CE techniques, although it may exhibit slow convergence. To avoid excessive processing time in practical systems, the sub-optimum Branch-and-Bound for Constellation Extension (BBCE) scheme is proposed. Simulation results show that BBCE achieves a significant PAPR reduction, providing a good trade-off between complexity and performance. We also show that the BBCE scheme performs satisfactorily in terms of Power Spectral Density (PSD) and Bit Error Rate (BER) in the presence of a non-linear High Power Amplifier (HPA).**

***Index Terms*—OFDM, peak power reduction, constellation extension, generalized benders decomposition, branch-and-bound**

I. Introduction

ORTHOGONAL Frequency Division Multiplexing (OFDM) is a modulation technique widely used in wireless communication systems due to its high data rate, strong immunity to multipath and high spectral efficiency. However, OFDM suffers from high Peak-to-Average Power Ratio (PAPR) of the transmitted signal. These large peaks introduce a serious degradation in performance when the signal passes through the non-linear zone of the High Power Amplifier (HPA) [7]. The non-linearity of the HPA leads to in-band distortion, which increases Bit Error Rate (BER), and out-of-band radiation, which causes adjacent channel interference.

M. C. Paredes Paredes is with the Department of Signal Theory and Communications, Universidad Carlos III de Madrid, Leganés, Madrid - Spain (e-mail: mcparedes@tsc.uc3m.es).

J. J. Escudero-Garzás is with the Department of Signal Theory and Communications, Universidad Carlos III de Madrid, Leganés, Madrid - Spain (e-mail: jescugar@tsc.uc3m.es).

M. J. Fernández-Getino García is with the Department of Signal Theory and Communications, Universidad Carlos III de Madrid, Leganés, Madrid - Spain (e-mail:mjulia@tsc.uc3m.es).

In the literature, there are several proposals to overcome the well-known PAPR problem, such as clipping, distortionless schemes and constellation extension (see [9], [11], [22] and references therein). Clipping is the simplest technique, but this process is non-linear and deteriorates the BER [2]. As an alternative, PAPR reduction can be achieved with distortionless schemes, such as SeLected Mapping (SLM) [5], Partial Transmit Sequences (PTS) [15], [16], [18], [25] and Tone Reservation (TR) [14], [26], [28]. The main disadvantage of these distortionless algorithms is that the useful data rate may be unfavorably decreased, and they can also require the transmission of side information to the receiver. On the other hand, methods based on Constellation Extension (CE) try to alter the constellation or insert new constellation points to suppress the peaks with multiple signal representation strategies. Techniques of this type are Tone Injection (TI) [6], [26], Active Constellation Extension (ACE) [13], metric-based CE, named Simple Amplitude Predistortion (SAP) [23], metric-based Symbol Predistortion [24], ACE based on Convex Optimization [27], [31] and Constrained Constellation Shapping (CCS) techniques [1], [17], [29], [30].

The key of CE techniques, also known as symbol predistortion techniques, is to intelligently move the constellation points, which are placed such that the PAPR is minimized while the minimum distance of the constellation is not affected, and no BER degradation is consequently experienced by the system. Moreover, there is no user's data rate loss because these methods do not require side information. Nevertheless, they introduce an increase in the energy per symbol. For TI techniques the basic idea is to increase the constellation size so that every point in the original basic constellation can be mapped onto several equivalent points in the expanded constellation [26]. The ACE scheme is presented in [13], where all symbols are extended but its computational burden is high. To alleviate this burden, in [23] and [24] a metric is defined to measure how much each input symbol contributes to large peaks, and the frequency-domain symbols with the highest metric values are selected to be predistorted with a predefined extension factor, called scaling factor in [23] and [24]. This metric-based algorithm saves energy (since only a subset of symbols are predistorted) and it avoids a high computational load by using the defined metric. However, its main drawback is that the size of the set of predistorted frequency-domain symbols and the scaling factor are chosen from a group of values suggested by the authors after empirical

search, what limits performance. Recently, a metric-based amplitude predistortion algorithm aided by orthogonal pilot symbols has been introduced in [21]. On the other hand, in CCS techniques the constellation points are modified to reduce the PAPR, although the use of these techniques imply some BER degradation. Within CCS techniques, some works formulate the PAPR minimization as a convex optimization problem [1], [17], [29], [30]. For example, in [1] the authors propose a scheme based on the Error Vector Magnitude (EVM), where the PAPR minimization is formulated as a Second Order Cone Program (SOCP) problem, subject to constraints on the EVM and power on free subcarriers. They use Interior Point Methods (IPM) to solve the SOCP. In [30], an iterative SOCP algorithm is proposed to achieve a quasi-constant PAPR. In [17], an EVM optimization framework is presented to deal with the PAPR problem, and a customized IPM is developed to solve the optimization problem. In [29] EVM minimization is formulated as a non-convex Quadratic Program (QP) utilizing SemiDefinite Relaxation (SDR), subject to constraints on PAPR and free subcarrier power overhead. In [27] and [31], the PAPR minimization is addressed following the SOCP approach. The authors of [27] propose the ACE-IPM scheme, which slightly reduces the theoretical complexity associated to the EVM-IPM of [1]. In [31], a generalized IPM-based method is also proposed. For the sake of clarity, in the sequel we refer to as CE techniques only when those techniques shift the outer constellation points toward allowed region.

In this paper, two novel CE-based algorithms for solving the PAPR problem are proposed. These algorithms determine both the adequate extension factor and the set of frequency-domain input symbols to be extended, *i.e.*, predistorted, per OFDM symbol. In our approach the PAPR minimization is formulated as a Mixed Integer Non-Linear Programming (MINLP) optimization problem. First, we employ a Generalized Benders Decomposition (GBD) method to find the optimum solution in terms of PAPR reduction. This scheme is called Generalized Benders Decomposition for Constellation Extension (GBDCE) and yields a relevant PAPR reduction. The GDBCE solution turns out to be a bound for CE schemes and provides a benchmark to compare with other CE techniques. However, GBDCE occasionally requires a large execution time mainly due to the fact that using GBD implies a sequential process to find the optimum solution.

In order to obtain a reduction in the execution time the sub-optimal Branch-and-Bound for Constellation Extension (BBCE) scheme is presented. The BBCE algorithm decreases the execution time by restricting the value of the extension factor to a set of discrete values. The processing time associated with both proposed schemes is analyzed in depth to determine the reduction in terms of execution time that BBCE provides with respect to GBDCE, what is closely related to complexity. Simulation results show that BBCE also achieves a significant PAPR reduction, providing a good trade-off between complexity and performance. We also show that the BBCE scheme performs satisfactorily in terms of Power Spectral Density (PSD) and BER in the presence of a non-linear HPA, for different values of Input Back-Off (IBO).

The remainder of this paper is organized as follows. Section II introduces the OFDM signal model and the PAPR definition. In Section III, the optimization problem is formulated. The optimum GBDCE algorithm is presented in Section IV. The sub-optimum BBCE scheme is proposed in Section V. The complexity analysis of both algorithms is discussed in Section VI. In Section VII our proposals are evaluated and compared with other CE schemes through simulations. Finally the conclusions are drawn in Section VIII.

II. PAPR definition in OFDM systems

An OFDM symbol is the sum of N independent signals modulated onto subchannels of equal bandwidth, which is efficiently implemented by an Inverse Discrete Fourier Transform (IDFT) operation. The time-domain transmitted signal for the ℓth OFDM symbol is given by:

$$b^{\ell}[n] = \frac{1}{\sqrt{N}} \sum_{k=0}^{N-1} a^{\ell}(k)\, e^{j2\pi kn/N} \quad , 0 \leq n < N-1 \quad (1)$$

where k and n are the frequency and time indices respectively, $a^{\ell}(k)$ is the complex data symbol transmitted over the kth subcarrier, $k = \{0, \ldots, N-1\}$ and $\mathbf{a}^{\ell} = \left[a^{\ell}(0) \ldots a^{\ell}(N-1)\right]$.

The data $a^{\ell}(k)$ are assumed to be independent, identically distributed (i.i.d.) random variables, and, based on the central limit theorem, the time-domain output samples follow an approximate complex Gaussian distribution with zero mean. Thus, the most samples will have low values but a small percentage of these samples will show very large peaks, due to the Rayleigh distribution of the envelope. This is the well-known PAPR problem. In general, the PAPR (denoted as χ^{ℓ}) of the time-domain samples $b^{\ell}[n]$ is defined as the ratio between the maximum instantaneous power and its average power [26]:

$$\chi^{\ell} = \text{PAPR}\left\{\mathbf{b}^{\ell}\right\} = \frac{\max\left|b^{\ell}[n]\right|^2}{E\left[\left|b^{\ell}[n]\right|^2\right]}, \quad 0 \leq n < N-1 \quad (2)$$

where $E[\cdot]$ denotes the expected value and $|\cdot|$ means modulo operation. A mathematically equivalent form to define the PAPR is [26]:

$$\chi^{\ell} = \text{PAPR}\left\{\mathbf{b}^{\ell}\right\} = \frac{\| \mathbf{b}^{\ell} \|_{\infty}^2}{E\left[\| \mathbf{b}^{\ell} \|_2^2\right]/N}, \quad (3)$$

where $\mathbf{b}^{\ell} = \left[b^{\ell}[0] \ldots b^{\ell}[N-1]\right]$ is an $1 \times N$ vector that collects the time-domain samples and $\| \cdot \|_p$ denotes the $p-$norm.

The most common way to evaluate the PAPR performance is through the Complementary Cumulative Distribution Function (CCDF), which determines the probability that the PAPR of a certain OFDM symbol goes beyond a fixed threshold (χ_0). Thus, the CCDF can be written as [20]:

$$\text{CCDF}\left(\chi^{\ell}\right) = Pr\left(\chi^{\ell} > \chi_0\right) = 1 - \left(1 - e^{-\chi_0^2}\right)^N. \quad (4)$$

III. Constellation Extension via Optimization

In this section we introduce the problem of PAPR minimization via constellation extension, and we reformulate it as an MINLP problem to exactly determine the optimal solution.

A. Problem formulation

As stated above, the basis of CE techniques is to shift the outer constellation points of the complex transmitted signal to combat large signal peaks. When the outer constellation points are moved within their external quadrant (see Fig. 1) the minimum distance between symbols is not affected. Moreover, the error margin is increased, which guarantees a lower BER. This idea is easily explained in the case of an OFDM system with Quadrature Phase-shift Keying (QPSK) modulation at each subcarrier, as shown in Fig. 1a, where the shaded region represents the allowed extension region. Note that, for constellation of higher order than QPSK such as 16-QAM (Quadrature Amplitude Modulation), the inner constellation points cannot be moved out without affecting the minimum distance, so they are not modified. This is illustrated in Fig 1b, where the constellation points are divided into three groups (inner points, boundary points and corner points) and they are only allowed to move in the directions indicated by the arrows. The complex symbol $a^{\ell}(k)$ is expanded to any point of the allowed region by adding an extension factor $c^{\ell}(k) \in \mathbb{C}$ and becomes the extended frequency-domain complex symbol $\bar{a}^{\ell}(k) = a^{\ell}(k) + c^{\ell}(k)$. The predistorted time-domain samples are given by:

$$\bar{b}^{\ell}[n] = \frac{1}{\sqrt{N}} \sum_{k=0}^{N-1} \left(a^{\ell}(k) + c^{\ell}(k) \right) e^{j2\pi kn/N}. \tag{5}$$

Mathematically, and in a very simplified formulation, the general PAPR minimization problem via CE can be expressed as:

$$\min_{\mathbf{c}^{\ell} \in C^{\ell}} \bar{\chi}^{\ell} = \min_{\mathbf{c}^{\ell} \in C^{\ell}} \frac{\max \left| \bar{b}^{\ell}[n] \right|^2}{E\left[\left| \bar{b}^{\ell}[n] \right|^2 \right]}, \tag{6}$$

where $\mathbf{c}^{\ell}$ represents the $1 \times N$ vector with extension factors $c^{\ell}(k)$ and C^{ℓ} is the constrained space of allowed extension vectors. We also define $\bar{\mathbf{b}}^{\ell} = \left[\bar{b}^{\ell}[0] \dots \bar{b}^{\ell}[N-1] \right]$ as the vector containing the predistorted time-domain samples.

We base our approach on the determination of the extension factors and the set S_L of those frequency-domain symbols to be predistorted. Consequently, S_L consists of those $a^{\ell}(k)$ such that their associated $c^{\ell}(k)$ are not null:

$$S_L = \{ a^{\ell}(k) \mid c^{\ell}(k) \neq 0 \}. \tag{7}$$

The cardinality of this set is L ($L = |S_L|$) and it is fulfilled that $L \leq N$. Determining S_L has been indirectly addressed in the recent CE literature. We next briefly present the most relevant techniques in this regard.

1) Active Constellation Extension (ACE): The ACE technique proposed in [13] is formulated for the ℓth OFDM symbol as the following min-max optimization problem:

$$\min_{\mathbf{c}^{\ell} \in C^{\ell}} \max_{n} \left| \bar{b}^{\ell}[n] \right|^2, \tag{8}$$

For convenience, instead of the additive extension factor $c^{\ell}(k)$, where $\bar{a}^{\ell}(k) = a^{\ell}(k) + c^{\ell}(k)$, a multiplicative extension factor $d^{\ell}(k) \in \mathbb{C}$ is preferred, where $\bar{a}^{\ell}(k) = a^{\ell}(k)\, d^{\ell}(k)$. This convention will be used from now on.

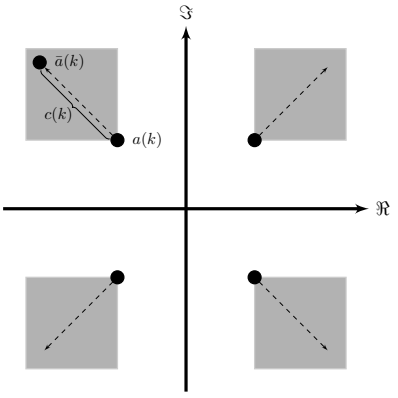

(a) Extension regions for QPSK constellation points.

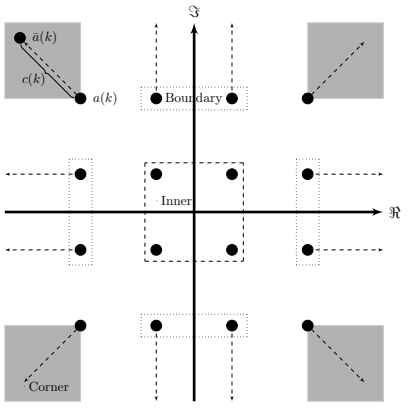

(b) Extension regions for 16-QAM constellation points

Fig. 1: These regions define the set of values that $\bar{a}(k) = a(k) + c(k)$ is allowed to take.

In the ACE approach all the constellation points can be expanded by an extension factor $d^{\ell}(k)$, with $|d^{\ell}(k)| \geq 1$. This technique can be characterized by the cardinality of S_L and the extension factors:

- Cardinality of S_L: $L \leq N$
- Extension factor: $\mathbf{d}^{\ell} = \left\{ d^{\ell}(k) \right\}_{k=0}^{N-1}$

where $\mathbf{d}^{\ell} \in D^{\ell}$ represents the $1 \times N$ vector with extension factors $d^{\ell}(k)$ and D^{ℓ} is the constrained space of allowed ACE vectors.

The optimization process is highly complex, specially because it requires an important number of iterations. To avoid this computational complexity one practical implementation of ACE technique is Projection onto Convex Sets (POCS), which is described in [13].

2) Simple Amplitude Predistortion (SAP): SAP is presented in [23], where the outer constellation points are modified by using a predefined extension factor $d^{\ell}(k) = \alpha \in \mathbb{R}$ ($|\alpha| \geq 1$) that is independent not only of the subcarrier index k but also of the OFDM symbol index ℓ, *i.e.* the same extension factor is applied to all subcarriers for all OFDM symbols. To determine S_L the algorithm uses a metric for each input data symbol that measures the input symbol contribution to the IDFT output

samples with large values, and then, the L symbols with the largest positive metrics are predistorted. Similarly to ACE, this technique can be described by

- Cardinality of S_L: $L < N$
- Extension factor: $\mathbf{d}^\ell = \alpha \mathbf{1}_{1\times N}$, where $\mathbf{1}_{1\times N}$ is the $1\times N$ all ones vector.

SAP is limited in performance since α is restricted to be fixed $\forall k, \ell$. Moreover, α and L are determined from a few suggested values $\alpha = \{1.3, 1.55, 2\}$ with $L = \{40, 26, 10\}$ respectively [23]. Indeed, only the elements of S_L are found out in real-time, because its cardinality L is chosen a priori. This simple scheme ensures a low-complex implementation but at the cost of a poor performance.

3) ACE based on IPM (ACE-IPM): In [27] the PAPR minimization is formulated as a SOCP problem and solved by using logarithmic-barrier IPM. In this case, the problem formulation is:

$$\begin{aligned} \min \quad & \max_n \left| b^\ell[n] \right|^2 \\ \text{s.t.} \quad & \mathbf{b}_{\text{R}}^\ell = [\Re\{\mathbf{b}^\ell\}, \Im\{\mathbf{b}^\ell\}] = \text{IFFT}(\mathbf{a}_{\text{v}}^\ell, \mathbf{a}_{\text{F}}^\ell) \\ & \text{sign}(\bar{a}_{\text{v}}^\ell(u) - a_{\text{v}}^\ell(u)) \times \text{sign}(\bar{a}_{\text{v}}^\ell(u)) \geq 0,\ u = 1, \ldots, U \end{aligned} \tag{9}$$

where $\mathbf{b}_{\text{R}}^\ell \in \mathbb{R}^{2N}$ is the vector containing the real and imaginary parts of $\mathbf{b}^\ell$, $\Re\{\cdot\}$ and $\Im\{\cdot\}$ represent the real and imaginary part, $\mathbf{a}_{\text{v}}^\ell \in \mathbb{R}^U$, $\mathbf{a}_{\text{F}}^\ell \in \mathbb{R}^{2N-U}$, and U is the total number of variables, *i.e.*, the number of constellation points suitable to be predistorted. In (9), the original frequency-domain symbols are classified into two groups: $\mathbf{a}_{\text{F}}^\ell$ is the vector representing the inner points (not allowed to be extended), and $\mathbf{a}_{\text{v}}^\ell$ is the vector representing the constellation points allowed to be predistorted (corner and boundary points). The resulting expanded constellation points are denoted by $\bar{\mathbf{a}}_{\text{v}}^\ell$. In accordance with the above characterization, the technique is defined by:

- Cardinality of S_L: $L \leq N$
- Extension factor: $\mathbf{d}^\ell = \{\bar{\mathbf{a}}_{\text{v}}^\ell - \mathbf{a}_{\text{v}}^\ell\}_{k=0}^{N-1}$.

B. Mixed Integer formulation for PAPR minimization

Regarding the PAPR problem, our objective is to determine the set of symbols S_L that will be predistorted and to obtain the numerical values corresponding to such predistortion. This implies that we reformulate the PAPR minimization problem in terms of binary variables as follows.

Minimizing the PAPR is equivalent to minimizing the numerator of (3) whether predistortion of symbols $\bar{\mathbf{b}}^\ell$ is considered [26]. Given that the square can be omitted in the minimization operation, we define the objective function $\tilde{\chi}^\ell = \|\bar{\mathbf{b}}^\ell\|_\infty$, and the optimization problem becomes:

$$\min_{\mathbf{d}^\ell \in D^\ell} \tilde{\chi}^\ell, \tag{10}$$

with

$$\bar{b}^\ell[n] = b^\ell[n] + \frac{1}{\sqrt{N}} \sum_{k\in S_L} \left(d^\ell(k) - 1\right) a^\ell(k)\, e^{j2\pi kn/N}, \tag{11}$$

where $b^\ell[n]$ is the time-domain sample sequence without predistortion. Problem (10) can be formulated in terms of binary variables, where $x^\ell(k)$ is 1 or 0 depending if $a^\ell(k)$ belongs or not to S_L, *i.e.*,

$$x^\ell(k) = \begin{cases} 1, & a^\ell(k) \in S_L \\ 0, & a^\ell(k) \notin S_L \end{cases} \tag{12}$$

Then, (11) becomes

$$\bar{b}^\ell[n] = b^\ell[n] + \frac{1}{\sqrt{N}} \sum_{k=0}^{N-1} x^\ell(k) \left(d^\ell(k) - 1\right) a^\ell(k)\, e^{j2\pi kn/N}. \tag{13}$$

To reduce complexity, we assumed that $d^\ell(k)$ are real and do not vary as a function of k: $d^\ell(k) = \alpha^\ell \in \mathbb{R}, \forall k$. Therefore, (13) becomes:

$$\bar{b}^\ell[n] = b^\ell[n] + \frac{\alpha^\ell - 1}{\sqrt{N}} \sum_{k=0}^{N-1} x^\ell(k)\, a^\ell(k)\, e^{j2\pi kn/N}. \tag{14}$$

However, for extension of constellations with higher order than QPSK, the indices of those symbols that are candidates to be predistorted must be known a priori, as shown in Fig. 1b. Accordingly, we redefine (14) to obtain (15), where I_p, B_R, B_I and C_p are, respectively, the subsets of symbols that belong to inner, boundary in real, boundary in imaginary and the corner constellations points.

Then, the PAPR problem can be formulated as the following minimization problem:

$$\min_{\mathbf{x}^\ell, \alpha^\ell} \tilde{\chi}^\ell \tag{16}$$

being $\mathbf{x}^\ell = \left[x^\ell(0) \ldots x^\ell(N-1)\right]$. Consequently, in accordance with the characterization given for the ACE, SAP and ACE-IPM techniques, our formulation is defined by:

- Cardinality of S_L: $L \leq N$
- Extension factor: $\mathbf{d}^\ell = \alpha^\ell \mathbf{1}_{1\times N}$.

For the sake of clarity, we omit the use of superscript ℓ in the sequel, since the optimal parameters $\{\mathbf{x}, \alpha\}$ are obtained per OFDM symbol.

The solution to the optimization problem given by (16) provides both the optimal value of the extension factor ($\alpha \in \mathbb{R}$) and which symbols must be predistorted, *i.e.*, when $x(k) = 1$, the symbol $a(k)$ is predistorted. This solution will be denoted with superscript $(\cdot)^*$, and it is given by $(\mathbf{x}^*, \alpha^*)$. Problem (16) is an MINLP problem as it involves integer ($\mathbf{x}$) and non-integer variables (α), and the optimization function is non-linear. This problem is optimally solved by means of the GBD method in the following section.

IV. Optimum GBDCE algorithm

In this section we propose the Generalized Benders Decomposition for Constellation Extension (GBDCE) algorithm to solve (16). The GBDCE algorithm is derived from the GBD algorithm, which is here shortly described and detailed in Annex A. GBD consists of generating two sequences of updated upper (non-increasing) and lower (non-decreasing) bounds that converge within a given ε in a finite number of iterations [8]. The sequence of upper bounds corresponds to solving subproblems in the real variables by fixing the integer variables; these subproblems are related to as *primal*

$$\bar{b}^{\ell}[n] = b^{\ell}[n] + \frac{1}{\sqrt{N}} \left(\sum_{k \in I_p} x^{\ell}(k)\, a^{\ell}(k)\, e^{j2\pi kn/N} + \sum_{k \in C_p} \alpha^{\ell} x^{\ell}(k)\, a^{\ell}(k)\, e^{j2\pi kn/N} + \sum_{k \in B_R} x^{\ell}(k) \left(\alpha^{\ell} \Re\{a^{\ell}(k)\} + j \Im\{a^{\ell}(k)\} \right) e^{j2\pi kn/N} + \sum_{k \in B_I} x^{\ell}(k) \left(\Re\{a^{\ell}(k)\} + \alpha^{\ell} j \Im\{a^{\ell}(k)\} \right) e^{j2\pi kn/N} \right), \quad 0 \le n < N-1. \tag{15}$$

problem. The lower bounds are similarly obtained by solving successive subproblems in the integer variables by fixing the real variables; these subproblems are related to as *master problem*.

The details of the GBDCE algorithm are provided next and illustrated through Fig. 2. The two following steps are executed at ith iteration, $1 \le i \le I$, where $I < \infty$ is the number of iterations reached. First, an integer solution $\hat{\mathbf{x}}_{i-1}$ is provided and the *primal problem* is solved in α for this $\hat{\mathbf{x}}_{i-1}$. This results in an upper bound $\tilde{\chi}_{UB,i}$ for the problem (16) as well as the value $\hat{\alpha}_i$ to be used to solve the *master problem*. Then, the resulting *primal problem* at this ith iteration is:

$$\tilde{\chi}_{UB,i} = \min_{\alpha} \|\bar{\mathbf{b}}\|_{\infty} \quad \text{s.t.} \quad \mathbf{x} = \hat{\mathbf{x}}_{i-1} \tag{17}$$

Note that the algorithm must be initialized with a solution $\hat{\mathbf{x}}_0$. We have empirically determined that $\hat{\mathbf{x}}_0 = \mathbf{0}_{1\times N}$ is a valid initial solution, where $\mathbf{0}_{1\times N}$ is the $1 \times N$ null vector.

Second, the *master problem* is solved in the integer variable $\mathbf{x}$ with $\alpha = \hat{\alpha}_i$ and we obtain $\tilde{\mathbf{x}}_i$. The solution to this problem is a lower bound $\tilde{\chi}_{LB,i}$ for the optimal solution of (16) that can be solved in this case by standard integer optimization algorithms such as Branch-and-Bound (BB) [4]. Notice that although GBDCE makes use of BB to calculate the $\tilde{\chi}_{LB}$, this GBDCE algorithm markedly differs from the BBCE scheme proposed in the next section. Therefore, the *master problem* to be solved is:

$$\tilde{\chi}_{LB,i} = \min_{\mathbf{x}} \|\bar{\mathbf{b}}\|_{\infty} \quad \text{s.t.} \quad \alpha = \hat{\alpha}_i \tag{18}$$

These two steps are iteratively applied until convergence is reached, *i.e.*, the condition $(\tilde{\chi}_{UB,i} - \tilde{\chi}_{LB,i}) < \varepsilon$ is satisfied, being ε the parameter that defines the convergence of the GBDCE. As the sequence of upper bounds $\{\tilde{\chi}_{UB,i}\}_{i=1}^{I}$ is non-increasing and the sequence of lower bounds $\{\tilde{\chi}_{LB,i}\}_{i=1}^{I}$ is non-decreasing, this guarantees that the difference $(\tilde{\chi}_{UB,i} - \tilde{\chi}_{LB,i})$ converges within ε and so does the algorithm, according to Theorem 1 of Annex A.

Determining the optimal solution to the PAPR problem by means of the GBDCE approach implies a sequential process to compute the real-valued variable $\alpha \in \mathbb{R}$ along with the calculation of the integer variables $\mathbf{x}$ until the difference between $\tilde{\chi}_{UB}$ and $\tilde{\chi}_{LB}$ is less than ε. Therefore, the GBDCE convergence depends on an adequate value of ε, so the higher the value of ε, the faster the convergence of the algorithm but at the expense of less accuracy in the solution, and conversely.

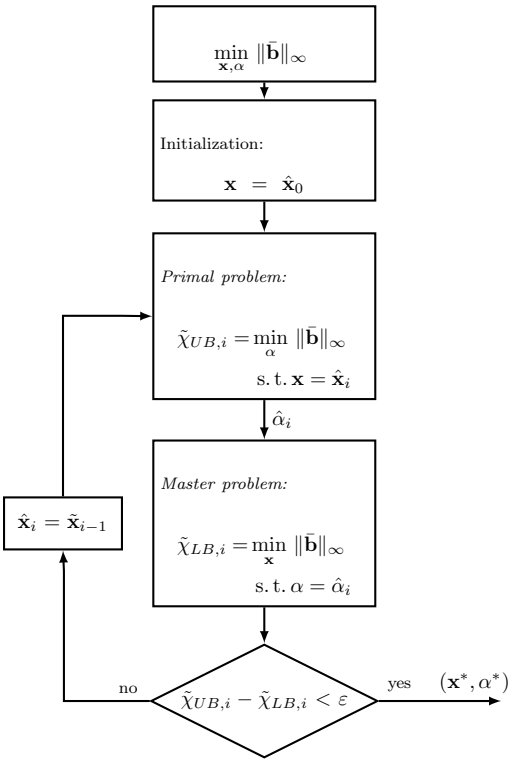

Fig. 2: Generalized Benders Decomposition for Constellation Extension (GBDCE) algorithm

V. Sub-optimum BBCE algorithm

The GBDCE scheme entails a significant computational complexity due to its sequential process. In this section we propose a sub-optimum algorithm named Branch-and-Bound for Constellation Extension (BBCE). This algorithm aims to alleviate the execution time associated with GBDCE and, at the same time, must guarantee convergence. Both objectives can be achieved if the value of α is restricted to a predetermined set of values given by $\mathcal{A} = \{1, 1+\delta, 1+2\delta, \ldots, 1+(Q-1)\delta\}$, being δ the step among consecutive values of α that defines the granularity in the accuracy of the solution, and Q is the cardinality of $\mathcal{A}$ ($Q = |\mathcal{A}|$).

The BBCE algorithm solves the PAPR problem given by (16) making use of a BB method as follows (see the flowchart of the algorithm in Fig. 3). BBCE finds the solution via Q-branch parallel computation, where at qth branch the following minimization problem is solved by means of a BB method,

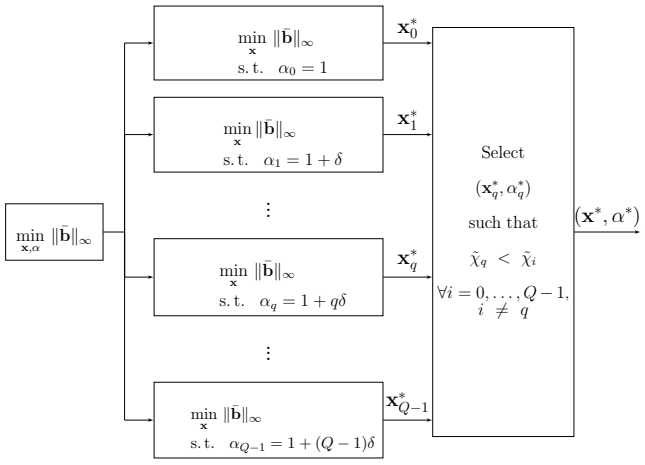

Fig. 3: Branch-and-Bound for Constellation Extension (BBCE) algorithm

yielding the solution $\mathbf{x}_q^*$:

$$\begin{aligned} &\min_{\mathbf{x}} \ \|\bar{\mathbf{b}}\|_\infty \\ &\text{s.t.} \quad \alpha = \alpha_q, \\ &\qquad q = \{0, \ldots, Q-1\} \end{aligned} \tag{19}$$

where $\alpha_q = 1 + q\delta$. Note that the number of branches is Q, *i.e.* each branch minimizes PAPR for a given value of $\alpha \in \mathcal{A}$. Thus, the problem (19) is solved in parallel as many times as determined by Q and at qth branch its associated $\tilde{\chi}_q$ is given by

$$\tilde{\chi}_q = \left[\|\bar{\mathbf{b}}\|_\infty\right]_{\mathbf{x}_q^*, \alpha_q}. \tag{20}$$

Finally, the solution $(\mathbf{x}^*, \alpha^*)$ corresponding to the lowest value within the set $S_\chi = \{\tilde{\chi}_q\}_{q=0}^{Q-1}$ is selected:

$$(\mathbf{x}^*, \alpha^*) = \underset{(\mathbf{x}_q, \alpha_q)}{\arg\min} \quad S_\chi \tag{21}$$

where $\min S_\chi$ is the minimum value within the set S_χ, denoted as $\tilde{\chi}^*$, and $(\mathbf{x}^*, \alpha^*)$ is the argument corresponding to $\tilde{\chi}^*$.

In terms of complexity, the key point is to define a set $\mathcal{A}$ as small as possible, which means a high granularity. As we decrease the value of delta $(\delta \to 0)$ we have a better approximation to the continuous case $\mathcal{A} = [1, Q] \in \mathbb{R}$, while for $\delta = 1$ the set reduces to Q points: $\mathcal{A} = \{1, \ldots, Q\}$. Then the higher the value of δ, the lower the processing time associated with the BBCE execution. With this in mind, we show through simulations in Section VII that the effect of increasing the granularity (δ) only has a slight impact on the PAPR performance. Hence $\mathbf{x}$ are the critical values of the BBCE scheme.

VI. Complexity Analysis

In this section we present the complexity analysis of our algorithms. First, we analyze our two algorithms (GBDCE and BBCE) in terms of execution time, and we show that the BBCE scheme is less complex than GBDCE. Second, we investigate the theoretical computational complexity and provide a comparison with other CE techniques.

A. Analysis of Execution time

The GBDCE algorithm provides the optimal solution to the PAPR problem. However, the execution time of this algorithm may be very large due to its sequential process. To effectively assess the difference in terms of execution time between GBDCE and BBCE, we characterize the execution time for both algorithms from a probabilistic point of view, as it is detailed next.

Let us denote the execution time per OFDM symbol with the random variable T, which accounts for the execution time due to processing the PAPR reduction technique via Matlab simulations. We have empirically observed that the histogram of the random variable T has a Rayleigh distribution (see Fig. 4). Consequently, the Probability Density Function (PDF) of T can be expressed as [19]:

$$f_T(t) = \frac{t}{\sigma^2} e^{-t^2/2\sigma^2} \quad , 0 < t \leq \infty \tag{22}$$

where σ is the parameter of the distribution. The value of σ can be estimated from M trials of the random variable as [19]:

$$\hat{\sigma} \approx \sqrt{\frac{1}{2M} \sum_{m=1}^{M} (t_m)^2}, \tag{23}$$

and the mean and variance of the Rayleigh distribution are respectively given by [19]:

$$E[T] = \left(\sqrt{\pi/2}\right)\sigma \tag{24}$$

$$Var[T] = (2 - \pi/2)\,\sigma^2. \tag{25}$$

The histograms in Fig. 4 represent the execution time for $N = 16$ and $N = 32$ subcarriers. In the x-axis of these figures we plot the execution time per OFDM symbol in [s], while y-axis provides the frequency. We represent in different scales the x-axis of the two algorithms in order to appreciate the Rayleigh envelope. Figs. 4a and 4c show the GBDCE execution time and Figs. 4b and 4d present the BBCE execution time for $\delta = 0.25$. These figures illustrate that the execution time of the GBDCE algorithm is higher than in the BBCE scheme.

The parameters of the Rayleigh distribution of each scheme are compared to confirm that BBCE algorithm requires less processing time. These parameters are summarized in Table I, in which we note that the mean and the variance of GBDCE for an OFDM system with $N = 32$ subcarriers are significantly larger than the values of BBCE. More specifically, the mean is almost triple and the variance is much higher, which implies that the Rayleigh distribution of the execution time of GBDCE scheme is more spread out, so we confirm again that GBDCE scheme is more expensive than BBCE in terms of processing time.

B. Computational Complexity

In the literature, we found some approaches that follow the idea of minimizing the PAPR through integer programming. For instance, ACE-POCS [13] shows that the complexity associated to the POCS method is $O(N \log N)$, where N is number of subcarriers. The complexity of a conventional

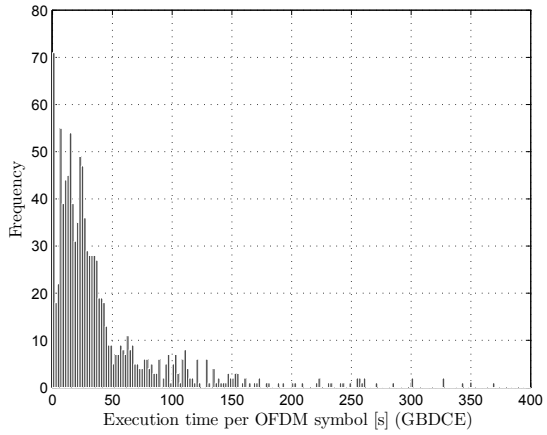

(a) Execution time of GBDCE technique for $N = 16$

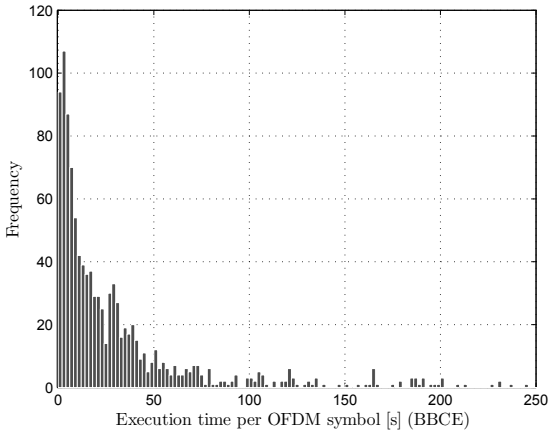

(b) Execution time of BBCE technique for $N = 16$

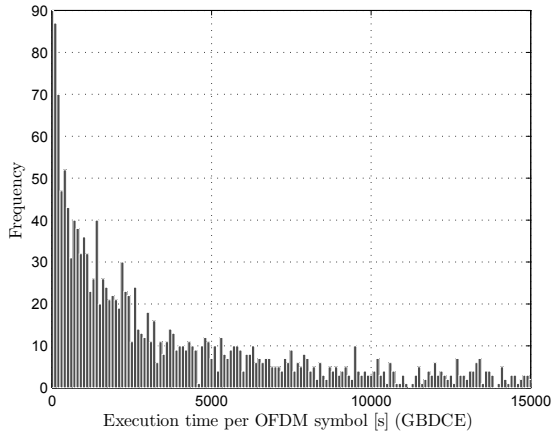

(c) Execution time of GBDCE technique for $N = 32$

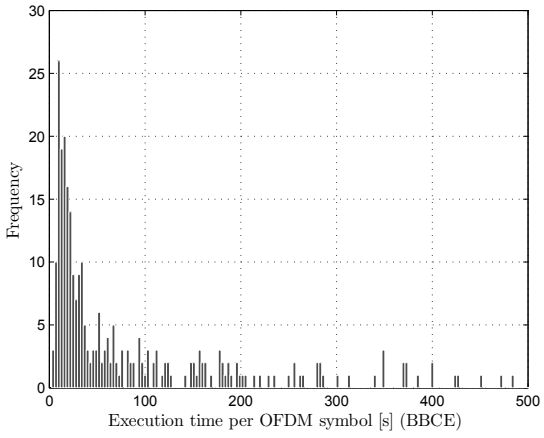

(d) Execution time of BBCE technique for $N = 32$

Fig. 4: Rayleigh distribution of the GBDCE and BBCE execution time per OFDM symbol with $N = \{16, 32\}$ subcarriers and QPSK modulations (Matlab simulation).

TABLE I: Summary of Rayleigh distribution parameters for an OFDM system with $N = \{16, 32\}$ subcarriers

Parameters	$N = 16$		$N = 32$	
	GBDCE	**BBCE**	**GBDCE**	**BBCE**
$\hat{\sigma}$	9.6	6.7	73.3	27.5
$E[T]$	12.1	8.3	91.9	34.5
$Var[T]$	39.9	19.2	2308.2	325.9

GBDCE algorithm is $O(IN \log N)$, where I is the number of iterations until the algorithm converges. Regarding the branch-and-bound algorithm that supports the BBCE algorithm, the associated complexity is $O(N \log N)$. It must be noted that the BBCE algorithm is parallely computed, so the Q branches are simultaneously solved. However, in our algorithms, we limit the extension to outer constellation points, which considerably reduces the complexity. We define $\Theta = \frac{M_{outer}}{M}$, where Θ represents the percentage of complex data symbols $a^{\ell}(k)$ susceptible to be expanded, and M_{outer} is the number of outer constellation points. For instance, if 16-QAM modulation is used, the four inner points cannot be extended, and the problem is solved in the twelve outer points of the constellation, *i.e.*, $\Theta = 12/16 = 0.75$. As the complex data symbols are independent, identically distributed (i.i.d.) random variables, Θ provides the percentage of assignment variables $x(k)$ that directly equal 0; for 16-QAM, this percentage is $(1 - \Theta) \times 100 = 25\%$. Hence, we have that the complexity for the GBDCE algorithm is $O(I\Theta N \log \Theta N)$, and the complexity associated to the BBCE algorithm is $O(\Theta N \log \Theta N)$. Clearly, $\Theta \leqslant 1$. Therefore, the BBCE algorithm exhibits lower complexity than the ACE-POCS.

With respect to CCS techniques proposed as convex minimization, the EVM-IPM algorithm [1] formulates the PAPR minimization as a SOCP, subject to constrained on EVM and power on free subcarriers. This problem entails $O(N^3)$ complexity. In [27], the authors present the ACE-IMP algorithm that slightly improves the theoretical complexity associated with the EVM-IPM algorithm, achieving a theoretical complexity of $O(I(2N + N^2))$, where I represents the number

of iterations used by the conjugate gradient algorithm. In the generalized IPM-based method [31], a specific constellation extension type is incorporated into the problem formulation as a set of convex functions. The proposed IPM algorithm is essentially the same that the ACE-IPM algorithm, with the difference that the optimal step size α must be calculated by solving an optimization problem (in ACE-IPM, α is given in closed form). Consequently, the complexity is larger than $O(I(2N+N^2))$, with an increase in the complexity given directly by that associated to the step size optimization problem. All these approaches have in common that a stopping criteria is required to terminate the algorithm, either in the form of maximum number of iterations or convergence of the solutions within a parameter ε.

Regarding the complexity of SAP [24], strictly speaking, it is a technique rather than an algorithm. This technique is useful to determine the predistortion level and the number of baseband symbols to be predistorted. As these two parameters are calculated offline through exhaustive simulations, no further modification can be done to these prefixed values and, consequently, the same values are applied to any transmitted OFDM symbol. Moreover, the calculated parameters are specific for a given number of subcarriers (FFT size) and modulation size. Said this, we consider that the complexity associated with the SAP technique should not be taken into consideration with respect to the algorithms proposed in our paper, as it is not an adaptive algorithm.

VII. Simulation Results

In this section, we provide the performance results for our GBDCE and BBCE algorithms, and they are compared with other CE schemes; more specifically, ACE-POCS [13], SAP algorithms [23] and ACE-IPM [27]. The performance of the PAPR reduction schemes is presented in terms of CCDF, Power Spectral Density (PSD) at the HPA, and BER at the receiver. Moreover, the convergence of the GBDCE algorithm is presented.

The results are obtained through Matlab simulations by averaging over 10^4 randomly generated OFDM symbols, for QPSK, 16-QAM and 64-QAM modulations, and different number of subcarriers $N = \{16, 32, 64, 128, 256\}$ are considered.

Fig. 5 shows the evolution of the difference between the upper and lower bounds at each iteration for $N = \{16, 32, 64\}$ subcarriers. We provide the initial points of $\tilde{\chi}_{UB} = 10^6$ and $\tilde{\chi}_{LB} = 0$, and the convergence parameter $\varepsilon = 10^{-6}$. Noticed that the GBDCE algorithm terminates when $(\tilde{\chi}_{UB} - \tilde{\chi}_{LB}) < \varepsilon$ is reached. From this figure, the fact that $\tilde{\chi}_{UB} - \tilde{\chi}_{LB}$ is close to 0 means that the GBDCE algorithm has converged in a finite number of iterations.

PAPR reduction techniques are applied whenever the PAPR of the OFDM symbol is greater than 6 dB, as it is usually specified [13]. In the figures, the solid marked green curves depict the GBDCE approach, the solid marked red lines show the BBCE technique. The solid line curves represent the performance for conventional OFDM signal without any PAPR reduction scheme; these curves are labelled as "Original" in all

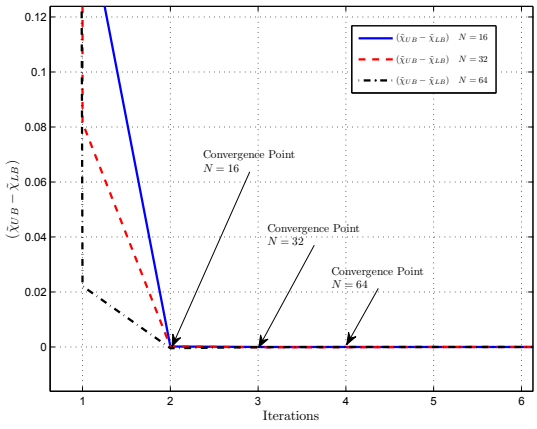

Fig. 5: Convergence of GBDCE algorithm: difference between the upper and lower bounds at each iteration for $N = \{16, 32, 64\}$ subcarriers and QPSK modulation.

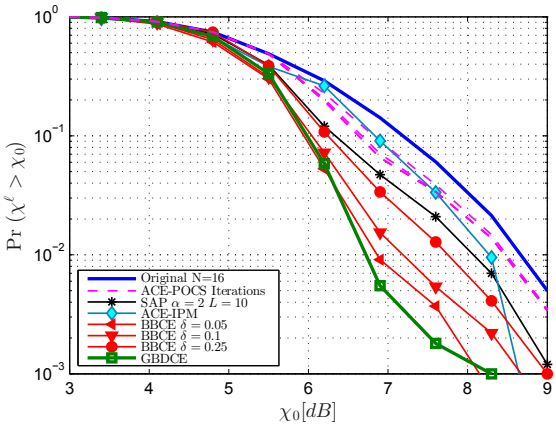

(a) OFDM system with $N = 16$ and QPSK modulation. BBCE with $\delta = \{0.05, 0.1, 0.25\}$

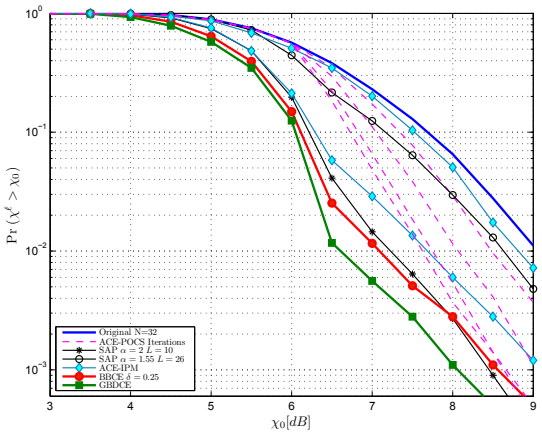

(b) OFDM system with $N = 32$ and 64-QAM modulation. BBCE with $\delta = 0.25$

Fig. 6: CCDF of PAPR for an OFDM system with $N = \{16, 32\}$. SAP with parameters set $\{L = 10, \alpha = 2\}$ and $\{L = 26, \alpha = 1.55\}$.

the subsequent figures. The dashed line curves correspond to ACE-POCS with iterations. Solid marked blue lines represent the ACE-IPM iterations, and the solid marked black lines show the SAP scheme.

The performance of GBDCE provides a lower bound for other PAPR reduction techniques in terms of CCDF. Figs. 6-8 show this fact for $N = \{16, 32, 64, 128, 256\}$ subcarriers, with QPSK, 16-QAM, and 64-QAM modulations. For instance, it is observed in Fig. 8 that the improvement of GBDCE at a probability of 10^{-2} is close to 4 dB with respect to the conventional OFDM signal without PAPR reduction. With respect to the above mentioned CE techniques, the minimum improvement of GBDCE is 1.4 dB.

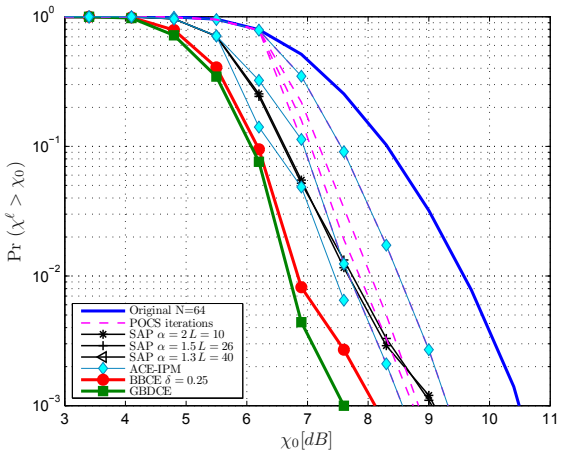

(a) OFDM system with $N = 64$ subcarriers

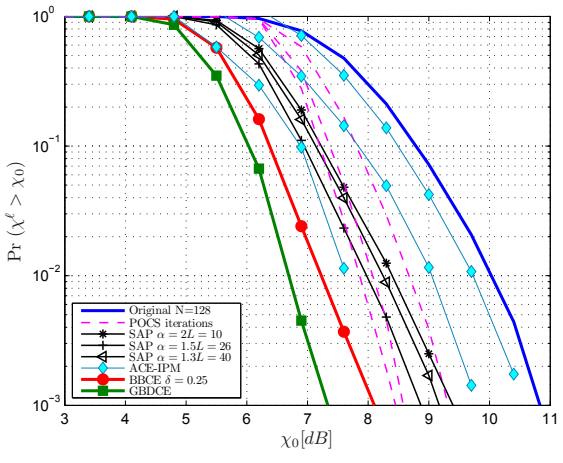

(b) OFDM system with $N = 128$ subcarriers

Fig. 7: CCDF of PAPR for an OFDM system with $N = \{64, 128\}$ and 16-QAM modulation. SAP with parameters set $\{L = 10, \alpha = 2\}$, $\{L = 26, \alpha = 1.55\}$ and $\{L = 40, \alpha = 1.3\}$ and BBCE with $\delta = 0.25$.

Regarding the BBCE algorithm, we first assess the impact of the granularity of the extension factor α given that the larger the value of δ, the lower the accuracy in α. Note that we impose the restriction $1 \leq \alpha \leq 2$ to avoid an excessive energy increase. Fig. 6a shows the performance of BBCE for an OFDM system with $N = 16$ subcarriers and QPSK modulation. We consider the set of values $\delta = \{0.05, 0.1, 0.25\}$. A small degradation in performance is observed when δ is increased, with a loss of 0.7 dB at a probability of 10^{-2} for the most unfavorable case of $\delta = 0.25$ with respect to GBDCE. At the same time, BBCE outperforms the other CE schemes. Therefore, we utilize the BBCE algorithm with $\delta = 0.25$ for the next simulation scenarios, given that the trade-off between execution time and performance is satisfactory. Figs. 6-8 confirm that BBCE performs better than the other CE-based techniques for larger number of subcarriers. For instance, for $N = 128$ subcarriers and 16-QAM modulation (see Fig. 7b), BBCE presents a reduction of approximately 2.8 dB at a probability of 10^{-2} with respect to the conventional OFDM signal. To evaluate the performance of the BBCE

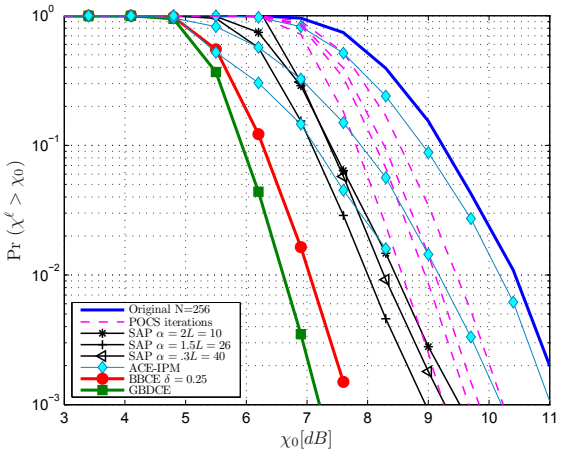

Fig. 8: CCDF of PAPR for an OFDM system with $N = 256$ and QPSK modulation. SAP with parameters set $\{L = 10, \alpha = 2\}$, $\{L = 26, \alpha = 1.55\}$ and $\{L = 40, \alpha = 1.3\}$ and BBCE with $\delta = 0.25$.

algorithm under complete transmitter operation, we verify the Power Spectral Density (PSD) observed at the input and output of a non-linear HPA. A common configuration is to use a Solid State Power Amplifier (SSPA), which can be modelled according to the modified Rapp's SSPA model [10], where the amplitude/phase (AM/PM) and amplitude/amplitude (AM/AM) characteristics are expressed as:

$$G\left(|b[n]|\right) = \frac{|b[n]|}{\left(1 + \left(|b[n]|/A_{sat}\right)^{2p}\right)^{\frac{1}{2p}}} \quad (26)$$

$$\Phi\left(|b[n]|\right) \approx 0 \quad (27)$$

being $G(\cdot)$ and $\Phi(\cdot)$ the AM/AM and AM/PM conversion functions respectively, $|b[n]|$ is the amplitude of the input HPA signal, p is a parameter that controls the smoothness of the characteristic (the smaller p, the smoother the characteristic) and A_{sat} is the saturation level of SSPA. Note that the AM/PM of SSPA is zero.[1] In this case, the Rapp's SSPA model introduces only AM/AM distortion, and the output signal of

[1]The effect of the AM/PM conversion is not exactly zero, but it is very small and thus it is not considered in the SSPA model.

the SSPA can be expressed as:

$$y[n] = G\left(|b[n]|\right)\, e^{\{j\theta([n])+\Phi(|b[n]|)\}}, \tag{28}$$

where $\theta\left([n]\right)$ is the phase of the input SSPA signal.

Figure 9 shows the PSD at the output of the SSPA for an OFDM system with $N = 64$, 16-QAM modulation and oversampling factor $J = 4$. The SSPA operates at different values of Input Back-off (IBO) $\{5, 8, 15\}$ dB. We choose $p = 2$, an adequate value in practice [12]. PSD is estimated by using the Welch's averaged periodogram method with Hanning window. The observed out-of-band radiation is primarily caused by the SSPA non-linearity, in particular for small IBO values. The BBCE scheme achieves a reduction of this out-of-band radiation with respect to the conventional OFDM signal without PAPR reduction technique (labelled as "Original") for the same value of IBO. For instance, the reduction of the out-of-band radiation when using BBCE is about 2 dB for IBO $= 8$ dB and, for larger values of IBO (*i.e.* 15 dB), the out-of-band radiation is just slightly reduced when BBCE is applied, as it is shown in Fig. 9.

We also evaluate our PAPR reduction technique (BBCE) to confirm that no significant BER degradation occurs when we transmit using a non-linear SSPA. The simulations setup contemplates the use of an OFDM system with $N = 64$ subcarriers over an Additive White Gaussian Noise (AWGN) channel and 16-QAM modulation without oversampling. The Signal-to-Noise Ratio (SNR) is defined as the ratio between the average signal power and the average noise power.

The SSPA with IBO $= \{5, 8, 15\}$ dB and $p = 2$ is considered for both conventional OFDM signal without PAPR reduction technique (labelled in the figure as "Original") and the BBCE scheme. Additionally, as a baseline, the BER curves corresponding to "Original" OFDM signal and BBCE using a linear amplifier, which does not cause any signal distortion, are also depicted. From Fig. 10 we observe a better performance of our BBCE scheme with respect to the "Original" signal in terms of BER. This is due to two factors: i) the constellation expansion performed by BBCE does not affect the minimum distance of the constellation (as it is shown in Fig. 1b); ii) the constellation expansion increases the energy of some constellations points, which leads to a lower BER. For instance, for IBO $= 5$ dB, the gain in SNR of the BBCE scheme is approximately 3 dB with respect to the "Original" to meet BER $= 10^{-3}$. We also see in Fig. 10 that the use of a non-linear SSPA inherently introduces some degradation in BER with respect to the linear amplifier, for both the BBCE scheme and the "Original" signal. As expected, the degradation decreases as the value of IBO increases; for BBCE, this degradation is about 2 dB for BER $= 10^{-3}$ when IBO $= 5$ dB and becomes almost negligible for IBO $= 15$ dB.

Additionally, we have compared our algorithms with CSS techniques, more specifically, EVM-IPM [1] and EVM-SDR [29], whose main characteristic is that they degrade the BER. In these simulations, shown in Fig. 11 for $J = 1$ (*i.e.*, no oversampling is used), we analyze the representative case of $N = 64$ subcarriers, with 52 subcarriers for user data and 12 subcarriers set to zero as in the simulation scenario used

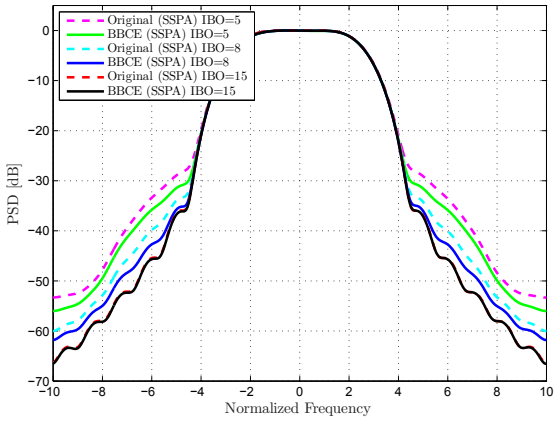

Fig. 9: PSD at the output of the SSPA without PAPR reduction (labelled as "Original") and BBCE with $N = 64$, 16-QAM modulation, $J = 4$ and $\delta = 0.25$.

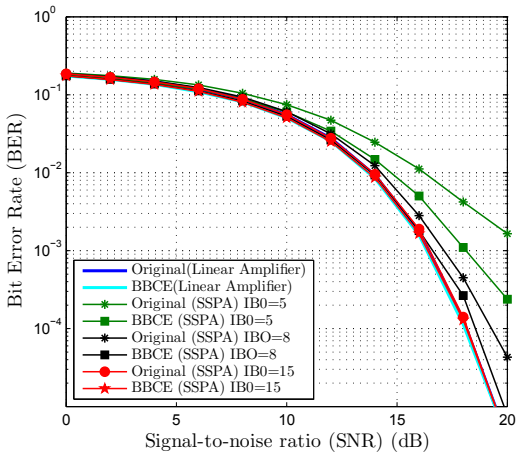

Fig. 10: BER performance of the BBCE scheme with $N = 64$, 16-QAM modulation, $J = 1$ and $\delta = 0.25$ over AWGN channel in the presence of a SSPA with IBO=$\{5, 8, 15\}$ dB.

in [1], [29]. Figure 11a shows that the BER performance is worse with CSS techniques. Figure 11b displays the CCDF performance, showing that the EVM-SDR scheme gains about 1 dB at a probability of 10^{-3} respect to GBDCE but at the expense of a degradation of more than 3dB in BER performance.

VIII. Conclusions

In this work, two novel CE-based algorithms are proposed to address the PAPR problem in OFDM systems. The GBDCE algorithm determines both the optimum extension factor and which complex symbols will be predistorted. Compared with other CE techniques, GBDCE provides a lower bound for the performance of CE techniques. For instance, for an OFDM system with $N = 256$ and using QPSK modulation, GBDCE provides an improvement close to 4 dB with respect to conventional OFDM signal without PAPR reduction, and a minimum improvement of 1.4 dB with respect to the considered CE

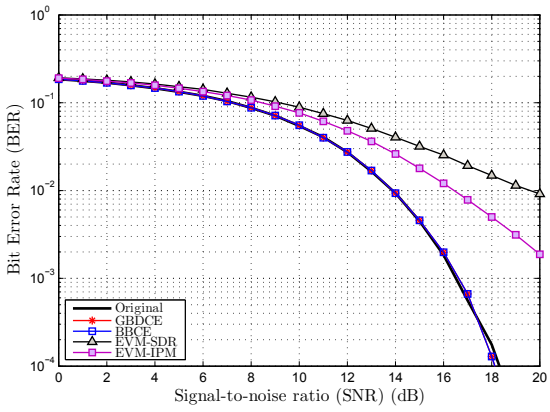

(a) BER performance for $N = 64$ subcarriers and 16-QAM modulation over AWGN channel

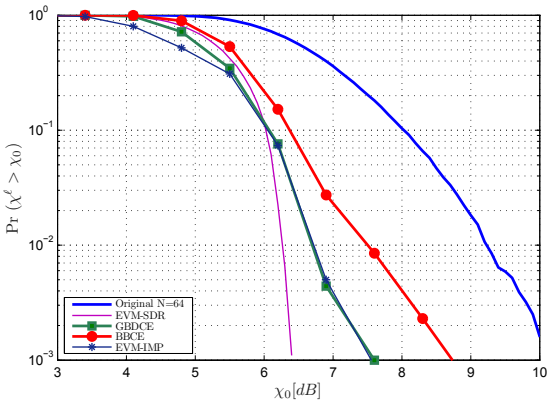

(b) CCDF for OFDM system with $N = 64$ subcarriers and 16-QAM modulation

Fig. 11: Comparison with CSS techniques. BBCE with $\delta = 0.25$, $J = 1$, EVM-IPM and EVM-SDR algorithms with -25dB of EVM tolerance and free subcarrier power overhead is 0.15 [29].

techniques at a probability CCDF $= 10^{-2}$. However, GBDCE may incur in slow convergence due to its sequential nature.

As a practical alternative, we propose the BBCE algorithm to reduce the excessive processing time that GBDCE may entail. The BBCE algorithm is based on restricting the extension factor to values within a discrete set at the expense of decreasing the accuracy of the extension factor. The sub-optimal BBCE scheme provides a good trade-off between complexity and performance. Besides, the BBCE scheme achieves a reduction of the out-of-band radiation caused by the HPA non-linearity and a better performance in BER with respect to the conventional OFDM signal.

A deep analysis of processing time for both algorithms reveals the reduction in terms of execution time of BBCE compared with GBDCE. We stress the relevance of this time analysis given that it is closely related to computational complexity.

Appendix A
General Benders Decomposition Algorithm

In his 1962 paper [3], Benders proposed an approach for exploiting the structure of optimization problems with complicating variables, *i.e.*, variables that make the optimization problem substantially more tractable once they have been fixed. This approach was generalized to non-linear problems by Geoffrion [8], who developed the Generalized Benders Decomposition (GBD) technique for problems of the form

$$\begin{aligned} \max_{\mathbf{x},\mathbf{y}} \quad & f(\mathbf{x},\mathbf{y}) \\ \text{s.t.} \quad & g(\mathbf{x},\mathbf{y}) \geqslant 0, \\ & \mathbf{x} \in \mathcal{X} \subset \mathbb{R}^N, \mathbf{y} \in \mathcal{Y} \subset \mathbb{R}^M, \end{aligned} \tag{29}$$

where $\mathbf{y}$ is a vector of complicating variables in the sense that (29) is much easier to solve in $\mathbf{x}$ when $\mathbf{y}$ is temporarily held fixed, N and M are positive integer values, and $g(\mathbf{x},\mathbf{y})$ is a vector of constrained non-linear functions. Therefore, GBD is suitable to solve situations in which, for fixed $\mathbf{y}$, problem (29) either separates into independent subproblems in $\mathbf{x}$ or assumes a well-known special structure.

The general ideas of the GBD can be summarized in the following steps:

1) (29) is projected onto $\mathbf{y}$:

$$\begin{aligned} \max_{\mathbf{y}} \quad & v(\mathbf{y}) \\ \text{s.t.} \quad & \mathbf{y} \in \mathcal{Y} \cap \mathcal{V}, \end{aligned} \tag{30}$$

where

$$v(\mathbf{y}) = \max_{\mathbf{x}} f(\mathbf{x},\mathbf{y}), \quad \text{s.t. } g(\mathbf{x},\mathbf{y}) \geqslant 0, \mathbf{x} \in \mathcal{X} \tag{31}$$

$$\mathcal{V} \triangleq \{\mathbf{y} : g(\mathbf{x},\mathbf{y}) \geqslant 0, \text{for some } \mathbf{x} \in \mathcal{X}\}, \tag{32}$$

with $\mathcal{Y} \cap \mathcal{V}$ representing the projection of the feasible region of (29) onto $\mathbf{y}$-space. Problem (30) is known as the *master problem*, and it is equivalent to the original problem (29) according to Theorem 2.1 of [8], with the advantage that evaluating $v(\mathbf{y})$ is considerably easier than solving (29). Problem (31) is denoted as the *primal problem* and it corresponds to solving (29) with fixed $\mathbf{y}$.

2) By invoking duality, the master problem can be formulated as

$$\begin{aligned} \max_{\mathbf{y}\in\mathcal{Y},\mathbf{y}_0} \quad & \mathbf{y}_0 \\ \text{s.t.} \quad & \mathbf{y}_0 \leqslant \sup_{\mathbf{x}\in\mathcal{X}} \{f(\mathbf{x},\mathbf{y}) + \boldsymbol{\mu} g(\mathbf{x},\mathbf{y})\}, \forall \boldsymbol{\mu} \geqslant 0 \\ & \sup_{\mathbf{x}\in\mathcal{X}} \{\boldsymbol{\lambda} g(\mathbf{x},\mathbf{y})\} \geqslant 0, \forall \boldsymbol{\lambda} \geqslant 0 \end{aligned} \tag{33}$$

3) Solving the relaxed master problem, *i.e.*, the master problem particularized in $\mathbf{x}^*$ which optimizes the primal problem, the optimal solution $\mathbf{y}^*$ provides the optimal value $\mathbf{y}_0^*$, which is an *upper bound* (UBD) of the optimal solution of the original problem (29).
4) Solving the primal problem for $\mathbf{y}^*$, the optimal solution $\mathbf{x}^*$ is updated and the optimal value $v(\mathbf{y}^*)$ is used to update the *lower bound* of the optimal value of (29) as $LBD = \min\{LBD, v(\mathbf{y}^*)\}$.

The successive application of steps 3 and 4 gives a sequence of upper and lower bounds. The sequence of upper bounds $\mathbf{y}_0^*$ is monotone and non-increasing. On the other hand, non-decreasing monotonicity is achieved for the sequence of lower bounds by constructing the lower bound as $LBD = \min\{LBD, v(\mathbf{y}^*)\}$, given that the sequence of optimal values $v(\mathbf{y}^*)$ needs not to be monotone decreasing. The optimal solution would be reached when $UBD = LBD$, although in practice an error parameter $\varepsilon = UBD - LBD$ is used. The above procedure or algorithm converges within a given ε, according to the following theorem [8].

Theorem 1: The Generalized Benders Decomposition algorithm terminates in a finite number of iterations for any given $\varepsilon > 0$ and even for $\varepsilon = 0$, if the following conditions hold:

- *$\mathcal{X}$ is non-empty and convex, and $f(\mathbf{x}, \mathbf{y}), g(\mathbf{x}, \mathbf{y})$ are convex for each fixed $\mathbf{y} \in \mathcal{Y} = \{0, 1\}$.*
- *The set $\mathcal{Z} = \{\mathbf{z} : g(\mathbf{x}, \mathbf{y}) \leqslant \mathbf{z}\}$ is closed for each fixed $\mathbf{y}$.*
- *For each fixed $\mathbf{y} \in \mathcal{Y} \cap \mathcal{V}$, one of the following two conditions hold:*
  1) *the original problem (29) has a finite solution.*
  2) *the original problem (29) is unbounded.*

ACKNOWLEDGEMENTS

This work has been partly funded by the Spanish National Projects GRE3N-SYST (TEC2011-29006-C03-03) and COMONSENS (CSD2008-00010), and SENESCYT (Ecuador).

REFERENCES

[1] AGGARWAL, A., AND MENG, T. Minimizing the Peak-to-Average power ratio of OFDM signals using Convex Optimization. *IEEE Transactions on Signal Processing 54*, 8 (Aug. 2006), 3099–3110.

[2] ARMSTRONG, J. Peak-to-average power reduction for OFDM by repeated clipping and frequency domain filtering. *Electronics Letters 38*, 5 (Feb. 2002), 246–247.

[3] BENDERS, J. Partitioning procedures for solving mixed-variables programming problems. *Numerische Mathematik 4*, 1 (1962), 238–252.

[4] BERTSEKAS, D. P. *Nonlinear Programming*. Athena Scientific, Belmont, MA, 1999.

[5] BÄUML, R., FISCHER, R., AND HUBER, J. Reducing the peak-to-average power ratio of multicarrier modulation by selected mapping. *Electronics Letters 32*, 22 (Oct. 1996), 2056–2057.

[6] DAMAVANDI, M. G., ABBASFAR, A., AND MICHELSON, D. G. Peak power peduction of OFDM systems through tone injection via parametric minimum Cross-Entropy method. *IEEE Transactions on Vehicular Technology 62*, 4 (May 2013), 1838–1843.

[7] DANILO-LEMOINE, F., FALCONER, D., LAM, C.-T., SABBAGHIAN, M., AND WESOLOWSKI, K. Power backoff reduction techniques for generalized multicarrier waveforms. *EURASIP Journal on Wireless Communications and Networking 2008*, 1 (2008), 437801.

[8] GEOFFRION, A. M. Generalized Benders Decomposition. *J. Optimization Theory and Applications 10*, 4 (1972), 237–260.

[9] HAN, S. H., AND LEE, J. H. An overview of peak-to-average power ratio reduction techniques for multicarrier transmission. *Wireless Communications, IEEE 12*, 2 (April 2005), 56–652.

[10] HONKANEN, M., AND HAGGMAN, S.-G. New aspects on nonlinear power amplifier modeling in radio communication system simulations. In *The 8th IEEE International Symposium on Personal, Indoor and Mobile Radio Communications (PIMRC)* (Sep. 1997), vol. 3, pp. 844–848.

[11] JIANG, T., AND WU, Y. An overview: peak-to-average power ratio reduction techniques for OFDM signals. *IEEE Transactions on Broadcasting 54*, 2 (June 2008), 257–268.

[12] KAITZ, T. Channel and interference model for 802.16b Physical Layer. *Contribution to the IEEE 802* (2001).

[13] KRONGOLD, B. S., AND JONES, D. L. PAR reduction in OFDM via active constellation extension. *IEEE Transactions on Broadcasting 49*, 3 (Sept. 2003), 258–268.

[14] KRONGOLD, B. S., AND JONES, D. L. An active-set approach for OFDM PAR reduction via tone reservation. *IEEE Transactions on Signal Processing, 52*, 2 (Feb. 2004), 495–509.

[15] LAIN, J.-K., WU, S.-Y., AND YANG, P.-H. PAPR reduction of OFDM signals using PTS: A real-valued genetic approach. *EURASIP Journal on Wireless Communications and Networking 2011*, 1 (2011), 126.

[16] LI, L., AND QU, D. Joint decoding of LDPC code and phase factors for OFDM systems with PTS PAPR reduction. *IEEE Transactions on Vehicular Technology 62*, 1 (June 2013), 444–449.

[17] LIU, Q., BAXLEY, R., MA, X., AND ZHOU, G. Error vector magnitude optimization for OFDM systems with a deterministic peak-to-average power ratio constraint. *IEEE Journal of Selected Topics in Signal Processing 3*, 3 (June 2009), 418–429.

[18] MÜLLER, S. H. AND HUBER, J. B. OFDM with reduced peak-to-average power ratio by optimum combination of partial transmit sequences. *Electronics Letters 33*, 5 (1997), 368–369.

[19] OCHI, M. *Applied probability and stochastic processes in engineering and physical sciences*. Wiley series in probability and mathematical statistics: Applied probability and statistics. Wiley, 1990.

[20] OCHIAI, H., AND IMAI, H. On the distribution of the peak-to-average power ratio in OFDM signals. *IEEE Transactions on Communications 49*, 2 (Feb. 2001), 282–289.

[21] PAREDES PAREDES, M. C., AND FERNÁNDEZ-GETINO GARCÍA, M. J. Energy efficient peak power reduction in OFDM with amplitude predistortion aided by orthogonal pilots. *IEEE Transactions on Consumer Electronics 59*, 1 (Feb. 2013), 45–53.

[22] RAHMATALLAH, Y., AND MOHAN, S. Peak-to-average power ratio reduction in OFDM systems: A survey and taxonomy. *IEEE Communications Surveys Tutorials 15*, 4 (Fourth Quarter 2013), 1567–1592.

[23] SEZGINER, S., AND SARI, H. OFDM peak power reduction with simple amplitude predistortion. *IEEE Communications Letters 10*, 2 (Feb. 2006), 65–67.

[24] SEZGINER, S., AND SARI, H. Metric-based symbol predistortion techniques for peak power reduction in OFDM systems. *IEEE Transactions on Wireless Communications 6*, 7 (July 2007), 2622–2629.

[25] SIEGL, C., AND FISCHER, R. F. H. Partial transmit sequences for peak-to-pverage power ratio reduction in multiantenna OFDM. *EURASIP Journal on Wireless Communications and Networking 2008*, 1 (2008), 325829.

[26] TELLADO, J. *Multicarrier modulation with low PAR: Applications to DSL and wireless*. Kluwer Academic Publishers, 2002.

[27] WANG, C., AND LEUNG, S. H. PAR reduction in OFDM through convex programming. In *IEEE International Conference on Acoustics, Speech and Signal Processing (ICASSP) 2008* (March 2008), pp. 3597–3600.

[28] WANG, L., AND TELLAMBURA, C. Analysis of clipping noise and tone-reservation algorithms for peak reduction in OFDM systems. *IEEE Transactions on Vehicular Technology 57*, 3 (May 2008), 1675–1694.

[29] WANG, Y.-C., WANG, J.-L., YI, K.-C., AND TIAN, B. PAPR Reduction of OFDM signals with minimized EVM via Semidefinite Relaxation. *IEEE Transactions on Vehicular Technology 60*, 9 (Nov. 2011), 4662–4667.

[30] WANG, Y.-C., AND YI, K.-C. Convex optimization method for quasi-constant peak-to-average power ratio of OFDM signals. *IEEE Signal Processing Letters 16*, 6 (June 2009), 509–512.

[31] YU, Z., BAXLEY, R., AND ZHOU, G. Generalized Interior-Point method for constrained peak power minimization of OFDM signals. In *IEEE International Conference on Acoustics, Speech and Signal Processing (ICASSP), 2011* (May 2011), pp. 3572–3575.

Martha Cecilia Paredes Paredes (S'12-M'15) received her Eng. degree from Escuela Politécnica Nacional (EPN), Quito, Ecuador in 2008, the M.Sc. and Ph.D of Multimedia and Communications from Carlos III University of Madrid, Spain in 2010 and 2014, respectively. Also, from 2010 to 2011 she worked as an Assistant Lecturer at Universidad de las Americas (UDLA), Quito - Ecuador. She is currently an Assistant Lecturer at Electronic, Telecommunication and Network Information Department (DETRI), EPN, Quito, Ecuador. Her research interests include multicarrier communications, OFDM transmissions and signal processing for wireless communications.

José Joaquín Escudero Garzás (S'06–M'10) received his Ph.D. degree in Electrical Engineering from the University Carlos III de Madrid (UC3M) in 2010. From 1997 to 2002, he worked for different Spanish telcos as a provisioning engineer and as head of the telecommunication network maintenance department. In 2002, he joined UC3M as an Assistant Lecturer. From October 2010 to September 2012, he was a postdoctoral fellow at the Dept. of Telecommunication and Systems Engineering of the Universitat Autònoma de Barcelona. He was also a Research Associate with the Dept. of Systems Engineering at University of Virginia (December 2012-November 2013). He is currently an Assistant Professor with the Dept. of Signal Theory and Communications, UC3M. His research interests include wireless communication systems and 5G networks.

M. Julia Fernández-Getino García (S'99 - AM'02 - M'03) received the M. Eng. and Ph.D. degrees in telecommunication engineering from the Polytechnic University of Madrid, Spain, in 1996 and 2001, respectively. She is currently with the Department of Signal Theory and Communications, Carlos III University of Madrid, Spain, as an Associate Professor. From 1996 to 2001, she held a research position with the Department of Signals, Systems and Radiocommunications, Polytechnic University of Madrid. She visited Bell Laboratories, Murray Hill, NJ, USA, in 1998; visited Lund University, Sweden, during two periods in 1999 and 2000; visited Politecnico di Torino, Italy, in 2003 and 2004; and visited Aveiro University, Portugal, in 2009 and 2010. Her research interests include multicarrier communications, coding and signal processing for wireless systems.

She received the best "Master Thesis" and "Ph.D. Thesis" awards from the Professional Association of Telecommunication Engineers of Spain in 1998 and 2003, respectively; the "Student Paper Award" at the IEEE International Symposium on Personal, Indoor and Mobile Radio Communications (PIMRC) in 1999; the "Certificate of Appreciation" at the IEEE Vehicular Technology Conference (VTC) in 2000; the "Ph.D. Extraordinary Award" from the Polytechnic University of Madrid in 2004; the "Juan de la Cierva National Award" from AENA Foundation in 2004; and the "Excellence Award" from Carlos III University of Madrid in 2012 for her research career.